Photoionization of the outer shells of radon and radium: Relativistic random-phase approximation for high-Z atoms

Pranawa C. Deshmukh
Department of Physics, Indian Institute of Technology, Madras 600 036, India

Vojislav Radojević
Department of Physics, Marmara University, 81040 Fikirtepe, Istanbul, Turkey

Steven T. Manson
Department of Physics and Astronomy, Georgia State University, Atlanta, Georgia 30303
(Received 20 November 1991)

Photoionization cross sections, branching ratios, and photoelectron angular distributions have been calculated for Ra ($Z=88$) $7s$, $6p$, $6s$, $5d$, and $5p$, and Rn ($Z=86$) $6p$, $6s$, $5d$, and $5p$ subshells within the framework of the relativistic random-phase approximation, including coupling between all of the relativistic channels arising from these subshells, in an effort to elucidate the interplay between relativistic and interchannel interactions at high Z where no experiments are extant. The results show that, aside from inducing structure in subshell cross sections, relativistic plus interchannel effects dominate the photoelectron angular-distribution asymmetry parameter and the branching ratio between spin-orbit doublets largely through the relativistic splitting of Cooper minima. This qualitatively confirms effects predicted by simple central-field calculations. Detailed explanations of the reasons for each of the structures are presented.

PACS number(s): 32.80.Fb

I. INTRODUCTION

Photoionization of high-Z atoms has been of considerable interest recently [1–6]. In addition to the applied importance of these studies, the high-Z atoms offer a laboratory to investigate the interplay of relativistic effects with the other atomic interactions and how this interplay manifests itself in the spectral distribution of oscillator strength. Simple calculations, based on the Dirac equation, have revealed interesting and unexpected effects connected with Cooper minima. The minima show large splittings, owing to relativistic effects, and these splittings have significant consequences for branching ratios and photoelectron angular distributions, in addition to the subshell cross sections [1–6].

Unfortunately, there is very little in the way of experiment for these high-Z atoms since many of them are radioactive. Thus, the predictions of the calculations have not been verified. In order to cast some light on the situation, we report here on the results of photoionization calculations of radon ($Z=86$) and radium ($Z=88$) using the sophisticated relativistic random-phase-approximation (RRPA) methodology [7,8], which includes exchange and a fair amount of correlation. In addition, the RRPA calculation has been shown to be quite excellent for photoionization of outer and near-outer subshells for lower-Z elements, particularly the noble gases [9,10]. The choices of Rn and Ra were dictated by the fact that RRPA is limited to closed-shell systems, in its present form.

In this paper, a comprehensive study of subshell cross sections and photoelectron angular-distribution asymmetry parameters is presented for Ra $7s$, $6p$, $6s$, $5d$, and $5p$ and Rn $6p$, $6s$, $5d$, and $5p$ subshells; we consider the outermost subshells of each. In the Ra calculation, 20 coupled relativistic dipole channels were employed, while 18 were used for Rn; these corresponded to all of the (relativistic) dipole allowed transitions from the subshells listed above. The energy range from threshold to the opening of the first omitted channel ($5s$) was considered.

The major thrust of this work is to test the predictions of simpler calculations of high-Z atomic photoionization both qualitatively and quantitatively. To that end, we have not dealt with the autoionizing resonances which occur below each threshold (other than the first threshold), nor the resonances between thresholds of spin-orbit doublets, but concentrate on the background (nonresonant) photoionization. It must be emphasized, however, that these resonances are implicitly included in the RRPA formalism, and they will be investigated in the future, by using RRPA in conjunction with relativistic multichannel quantum-defect theory (MQDT).

II. RESULTS AND DISCUSSION

In addition to studying the individual atoms Rn and Ra, by looking at both we can get some idea of the Z dependence of the various photoionization parameters. To that end, the results are discussed by subshell, rather than by element, going in from the outermost; note, of course, that only Ra has a $7s$ subshell. Unfortunately, no experimental data are available yet on the photoionization of such heavy atoms.

Before proceeding to the detailed discussion, it is useful

TABLE I. The Dirac-Fock threshold energies for radium (Ra) and radon (Rn) in atomic units (a.u.=27.21 eV).

Level	Ra	Rn
$7s$	0.17	
$6p_{3/2}$	0.74	0.38
$6p_{1/2}$	0.97	0.54
$6s$	1.62	1.07
$5d_{5/2}$	2.90	2.02
$5d_{3/2}$	3.12	2.19
$5p_{3/2}$	6.37	5.18
$5p_{1/2}$	7.84	6.41

to recall some facts about Cooper minima [11]. These are zeros in the dipole matrix elements and are found in ground-state atoms for $l \rightarrow l+1$ transitions in outer and near-outer subshells, provided the initial-state radial wave function is not nodeless. These zeros, in addition, are a very general phenomenon, occurring for almost all atoms heavier than neon [12–15]. Under the action of relativistic effects, a single zero becomes three zeros (two for initial s states), e.g., $p \rightarrow d$ becomes $p_{3/2} \rightarrow d_{3/2}$, $p_{3/2} \rightarrow d_{5/2}$, and $p_{1/2} \rightarrow d_{3/2}$; the $p_{1/2} \rightarrow d_{5/2}$, transition is forbidden since $\Delta j = 2$. Now zeros are very sensitive to any perturbation. Thus, scrutiny of these zeros is an excellent monitor of relativistic effects.

In previous work, it was found that the energies at which the zeros, arising from a single nonrelativistic zero, occurred showed very large splittings compared to the splitting of the initial states [11–16]. In order to discuss this point, in Table I, the theoretical Dirac-Fock binding energies of the initial states considered in this study are given.

A. 7s subshell

The results for the Ra $7s$ cross section are shown in Fig. 1, where the complexity as a function of energy is clearly seen. The cross section above shows minima at photon energies of about 0.4, 1.8, and 5.2 a.u., which appear in both length and velocity results. Note, however, that the agreement between length and velocity, which is excellent near threshold, gradually degrades with increasing $h\nu$. This is a general trend, as shall be clear in the discussion of subsequent subshells. Evidently, this gradual degradation is connected with our truncation of the RRPA calculation; the omission of the photoionization channels arising from the inner shells. The degradation becomes more pronounced as the photon energy approaches the energy at which the omitted channels open.

The origin of the structure in the $7s$ cross section can be traced to interchannel coupling. If only the $7s$ channels are included, the cross section is smooth and monotonically decreasing in the low-energy region; only the high-energy Cooper minima appear [16]. More specifically, the structure below 1 a.u. is due to interchannel coupling with the $6p$ channels, while the minimum just below 2 a.u. is caused by coupling with the $5d$ channels. Thus, the origin of the high-energy minimum, on the one hand, and the two low-energy minima, on the other, are rather different, the first arising in a single-channel calculation while the others are a result of correlation in the form of interchannel coupling. But does this mean that there are physical differences between the two kinds of minima? In other words, do the minima produced via interchannel coupling involve the change of sign of the dipole matrix elements which is characteristic of a Cooper minimum? Our results show that the answer is yes—each of the minima show a sign change in the matrix element. Thus, there is no real difference in the "intrinsic" and "induced" Cooper minima; the seeming difference results simply from thinking in terms of a single-electron picture.

For an s subshell in a closed-shell atom, the photoelectron angular-distribution asymmetry parameter β is independent of energy and equal to 2, in the absence of relativistic (spin-orbit) interactions [17]. Looking at Fig. 1, it is clear that β is not constant, indicating that spin-orbit forces are indeed important. Furthermore, there are significant dips in β, which come close to the lowest pos-

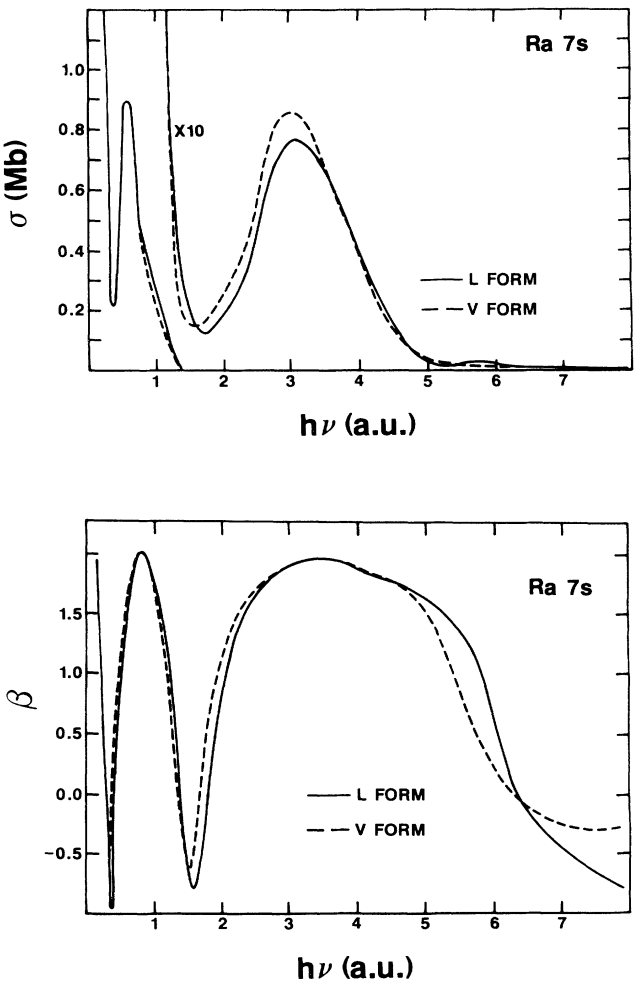

FIG. 1. Photoionization cross section and photoelectron angular-distribution asymmetry parameter β for Ra $7s$, calculated in a 20-channel RRPA in dipole-length (L) and dipole-velocity (V) formulations.

sible value of -1, near each of the minima, an additional indication that they are all of the same character. Such dips are expected in any s-state photoionization in the vicinity of Cooper minima and have been seen in a number of cases previously [17,18]. Basically, the behavior of β is due to the interaction between the $7s \rightarrow \epsilon p_{1/2}$ and $7s \rightarrow \epsilon p_{3/2}$ channels; the expression for β, in this case, is given by [17]

$$\beta = \frac{2R_{3/2}^2 + 4R_{1/2}R_{3/2}\cos(\delta_{1/2} - \delta_{3/2})}{R_{1/2}^2 + 2R_{3/2}^2} , \quad (1)$$

where the R_j are the dipole matrix elements to the ϵp_j continua and the δ_j are the phase shifts. For continuum electrons the spin-orbit interaction is small and the phase shifts are extremely close together so the cosine is quite close to unity. Then, if the two matrix elements are approximately equal, it is seen from Eq. (1) that $\beta \approx 2$. This will not be the case near the Cooper minimum where the two channels have their minima at different energies; $\beta = 0$ when $R_{3/2} = 0$ and $\beta = 1$ when $R_{1/2} = 0$. Furthermore, when the ratio of $R_{1/2}$ to $R_{3/2}$ is -2, which means that the matrix elements have different signs, Eq. (1) shows that $\beta = -1$.

In Fig. 1, it is seen that the dips in β approach, but do not quite hit, -1. This is because the discussion of the previous paragraph is not strictly true for a calculation which includes interchannel coupling. In such a calculation, the matrix elements are complex and the real and imaginary parts vanish at *slightly* different energies so that they never truly vanish; the matrix elements come close enough to zero for all practical purposes, however.

Note also in Fig. 1 that away from the minima, the value of β tends toward 2, as expected by the above discussion. It is also expected that at energies well above the high-energy minimum, β will again tend toward 2. We also see, in Fig. 1, the gradual degradation of agreement between length and velocity, with increasing energy, just as was the case for the cross section.

B. 6p subshells

The total photoionization cross sections for the 6p subshells of Ra and Rn are given in Fig. 2, where it is seen that they are rather high at its threshold and decrease steeply with the increase of photon energy; note that Ra 6p is not shown quite back to threshold, but its behavior is substantially the same as Rn 6p which is shown. Nevertheless, one must remember that close to the first threshold, there are strong electron correlations between the photoelectron and the residual ion, not all of which are properly accounted for by the RRPA. Relaxation effects not included in the present study also may be significant in this energy region. It is also seen that the effect of interchannel coupling quickly becomes an important factor as photon energies increase, and it is manifested as a pronounced hump in the 6p cross sections for both radium and radon just above their 5d thresholds, indicating that these structures are due to coupling with the 5d channels.

As discussed above, single Cooper minima for p states are split into three under the influence of relativistic effects. In both of the 6p cases there are two sets of Cooper minima. The minima in the 2-a.u. range, which show up clearly in Fig. 2, are "induced" minima which come about due to interchannel coupling with the 5d channels, just as subsequent humps are caused. In addition, there is a high-energy set in each case of minima which, due to the extent of their splitting, do not show up in the total subshell cross sections; these high-energy minima are, however, "intrinsic" minima.

The effects of these minima are, nevertheless, very evident in β. Roughly speaking, β should be zero when the $p \rightarrow d$ matrix element vanishes; physically, this is due to the fact that the cross section is then only $p \rightarrow s$ and an s state in entirely isotropic which corresponds to $\beta = 0$. This, of course, is not strictly true of the relativistic case owing to the splitting of the channels, but it still gives us a useful tool to analyze the approximate location of Cooper minima.

The β is shown in Fig. 3 for 6p of Ra and Rn, respectively. To begin with, dips are seen in β for Ra at about

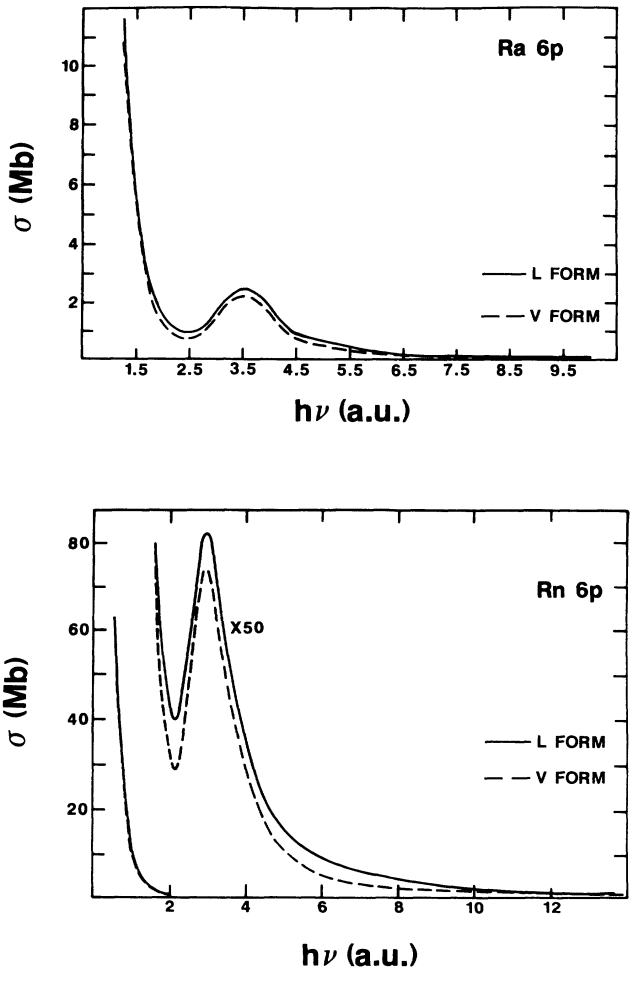

FIG. 2. Photoionization cross section for Ra 6p calculated in a 20-channel RRPA and Rn 6p calculated in an 18-channel RRPA in dipole-length (L) and dipole-velocity (V) formulations.

2.5 a.u. and for Rn at about 2 a.u., with β passing through the value of zero in each case. These dips correspond to the "induced" minima seen in Fig. 2, giving further indication that there are no physical differences between "induced" and "intrinsic" minima. As was the case for the cross sections in the same energy range, these dips in β are produced through interchannel coupling with the $5d$ channels. The rapid variation of β in this neighborhood indicates a rapid variation of individual matrix elements due to the interchannel coupling. Both $6p_{1/2}$ and $6p_{3/2}$ are seen to be affected significantly, and in the same energy range, by the interchannel coupling, although some differences are certainly seen; evidently the relativistic splitting of minima is not important here.

At higher energies, however, the β's are seen to exhibit broad shallow minima, the result of the "intrinsic" Cooper minima mentioned above. More importantly, for each element they are considerably shifted from one another in energy. Looking at the matrix elements for Rn $6p$, we find that the Cooper minima in the $6p_{3/2}\rightarrow\epsilon d_{5/2}$, $6p_{3/2}\rightarrow\epsilon d_{3/2}$, and $6p_{1/2}\rightarrow\epsilon d_{3/2}$ channels are at photon energies of about 7.38, 7.17, and 12 a.u., respectively.

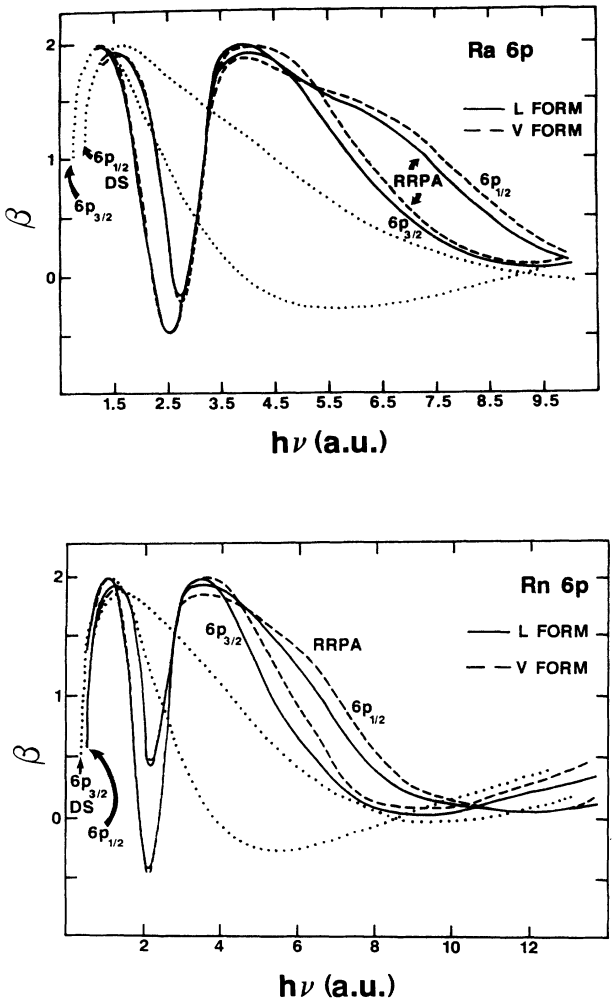

FIG. 3. Photoelectron angular-distribution asymmetry parameter β for $6p_{3/2}$ and $6p_{1/2}$ of Ra calculated in a 20-channel RRPA and Rn calculated in an 18-channel RRPA in dipole-length (L) and dipole-velocity (V) formulations. The dotted curves are the DS results of Ref. [4].

This splitting is essentially due to the relativistic spin-orbit interaction, so one may be tempted to believe, for example, that the energy spacing between the Cooper minimum in the $6p_{3/2}\rightarrow\epsilon d_{3/2}$ and $6p_{1/2}\rightarrow\epsilon d_{3/2}$ channels, for which the final continuum state is of the same angular symmetry, may correspond directly to the spin-orbit splitting of the $6p$ levels. The first theoretical calculations on this phenomenon made in the Dirac-Slater (DS) approximation showed that the energy splitting between the Cooper minima in the $6p_{3/2}\rightarrow\epsilon d_{3/2}$ and $6p_{1/2}\rightarrow\epsilon d_{3/2}$ channels is many times larger than the spin-orbit splitting of the $6p$ level. That this was not an artifact of the Dirac-Slater model was shown in a preliminary study of radon using the RRPA. The splitting of the $6p_{3/2}\rightarrow\epsilon d_{3/2}$ and $6p_{1/2}\rightarrow\epsilon d_{3/2}$ minima for Rn $6p$ is found to be 4.83 a.u. which is more than 30 times the spin-orbit splitting of the $6p$ levels, as seen from Table I. A detailed explanation for this magnification effect has been given elsewhere [3]. Roughly speaking, however, the splitting occurs because the $6p_{1/2}$ subshell has a greater binding energy than the $6p_{3/2}$, due to the spin-orbit effect, and thus its wave function is more compact. In the dipole matrix elements, the ϵd final continuum states, which move in toward the nucleus with increasing energy, the condition for a minimum is reached for the less compact $6p_{3/2}$ first, if we start from threshold and increase the energy. With increasing energy, the condition for a $6p_{1/2}$ minimum is reached, but this energy must be much larger than the $6p$ spin-orbit splitting owing to the centrifugal barrier. In other words, a given amount of energy (the spin-orbit splitting) is required to move the $6p_{3/2}$ in to the $6p_{1/2}$, but to move the ϵd in that same distance requires a much larger energy since it is "climbing" a centrifugal barrier three times as high as for the p states. Thus, the magnification effect occurs.

The size of this splitting, as well as the difference between the $6p_{1/2}$ and $6p_{3/2}$ β's, was seen to increase with Z in the range $Z=82$ to 100 in the Dirac-Slater calculation. This is seen to be true from Fig. 3, even in the vicinity of $5d$ thresholds where interchannel coupling occurs. These deviations are pronounced in the vicinity of the $5d$ thresholds, but as photon energy goes past the $5d$ thresholds, the β's rise to about 2 for both Ra and Rn. The subsequent fall in β for $6p_{3/2}$ is steeper than $6p_{1/2}$, which is certainly due to the fact that the dominant $p\rightarrow d$ matrix element goes through a Cooper minimum at a lower energy in the case of $6p_{3/2}$ than for $6p_{1/2}$. This is easily understood by recognizing that as the $6p_{1/2}\rightarrow\epsilon d_{3/2}$ matrix element goes to zero at its Cooper minimum, so does β for $6p_{1/2}$ at this energy, resulting in a gradual decrease in β for $6p_{1/2}$ from about 2. A similar consideration applies to the $6p_{3/2}$ case, which is however more complex because of the presence of the $p_{3/2}\rightarrow d_{5/2}$ as well as the $p_{3/2}\rightarrow d_{3/2}$ channels.

It is also evident that for both Ra and Rn, length and velocity results are substantially the same for both cross sections and β's. One does, however see a *slight* degrada-

tion of the agreement between length and velocity, indicating a slight effect of the truncation of the RRPA calculation, i.e., the omission of all of the channels from $5s$ and below.

Also shown for comparison in Fig. 3 are the β's resulting from the DS calculation [4]. DS and RRPA β's are quite similar near threshold (except for the differences in thresholds) for both Ra and Rn, but above the first maximum, the RRPA β's differ both quantitatively and qualitatively from the DS results. Just above the first maximum, the RRPA β's are dominated by the "induced" minimum due to the interchannel interaction with the $5d$ channels, as discussed above, but this interaction is not included in the DS formalism. At the higher energies, the minima are very sensitive to the details of the initial- and final-state wave functions. While interchannel effects are not terribly important here, exchange effects are. DS treats exchange only approximately and this approximate exchange remains the same in initial discrete and final continuum states. Thus, the Cooper minima are considerably shifted between DS and RRPA. Since the β's are so sensitive to the positions of the minima, the RRPA and DS results differ considerably in this region for both Ra and Rn. Note, however, that above the minimum region, the DS and RRPA β's begin to come together, as can be seen clearly in Fig. 3, for Rn. Finally, note that the DS results also correctly predict a significant relativistic splitting in the Cooper minima but a somewhat larger one than is predicted by RRPA, as seen from the splitting of the $6p_{1/2}$ and $6p_{3/2}$ β's in Fig. 3.

Relativistic and interchannel effects also play significant roles in the $6p_{3/2}$:$6p_{1/2}$ branching ratio γ which is shown for Ra and Rn in Fig. 4. The outstanding feature of these results is that, in both cases, γ is strongly energy dependent and substantially different from the statistical ratio of 2 over the entire photon energy range studied. For both cases, γ is generally much below the statistical ratio at low energies, and much above at the higher proton energies. Furthermore, a slight dip followed by a hump is seen, in each case, in the vicinity of the $5d$ thresholds.

The behavior of the γ's can be traced to a number of individual effects. To begin with, there is the relativistic kinetic-energy effect [19] which occurs because photoelectrons from the $6p_{1/2}$ and the $6p_{3/2}$ will have different kinetic energies, for the same $h\nu$. Thus, even if the two cross sections have exactly the same energy dependence, as a function of photoelectron energy, the $6p$ spin-orbit splitting gives rise to a nonstatistical branching ratio. Since the $6p$ cross sections for Ra and Rn are decreasing as a function of energy in the threshold region, and $6p_{1/2}$ is more tightly bound than $6p_{3/2}$, then the fact that γ contains a $6p_{3/2}$ cross section at a larger photoelectron energy than $6p_{1/2}$ means that γ should be below statistical. This is certainly the case as seen in Fig. 4. The dip and subsequent hump are due to the minima induced by the interchannel interaction with the $5d$ channels. Clearly, the $6p_{3/2} \rightarrow \epsilon d_{3/2,5/2}$ channels have their minima at lower energies, causing γ to dip for both Ra and Rn; at a slightly higher energy, the $6p_{1/2} \rightarrow \epsilon d_{3/2}$ minimum occurs which makes the $6p_{1/2}$ cross section anomalously small and causes the rise in each case. Above the hump, γ again drops, owing to the fact that the $6p_{3/2}$ cross section is dropping toward its intrinsic minima in each case. At higher energies, the $6p_{1/2} \rightarrow \epsilon d_{3/2}$ minimum occurs, which dramatically decreases the denominator and increases γ, as seen in Fig. 4. Thus, the location of Cooper minima, along with the kinetic-energy effect, are the principal determinants of the γ's.

The $6p$ branching ratios calculated in the Dirac-Slater approximation are also shown in Fig. 4. There is an overall qualitative agreement between the DS and the RRPA results. The structure resulting in a hump in the branching ratio in the neighborhood of the $5d$ thresholds, seen in the RRPA calculations, is naturally absent in the DS calculations since the interchannel couplings are not included in the DS calculation. Curiously, however, the peak in the hump in the $6p$ branching ratio is seen to be just below the $5d$ thresholds in the case of Ra, whereas in

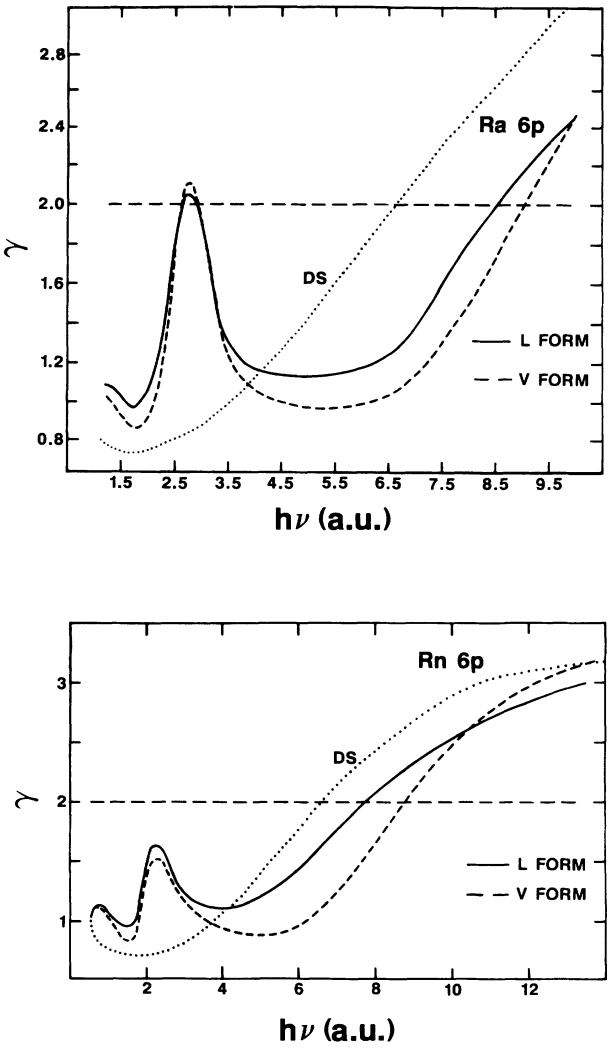

FIG. 4. $6p_{3/2}$:$6p_{1/2}$ branching ratio γ for Ra $6p$ calculated in a 20-channel RRPA and Rn $6p$ calculated in an 18-channel RRPA in dipole-length (L) and dipole-velocity (V) formulations. The dashed line is the statistical ratio of 2.0.

the case of Rn it is just above the $5d$ thresholds, showing that the details of the interchannel coupling are complex indeed.

C. 6s subshells

The cross sections for the $6s$ subshells are presented in Fig. 5 where complex behavior, as a function of energy, is seen. For both Ra and Rn, the cross section drops from threshold to an induced minimum caused by interchannel coupling with $5d$. Above this minimum is a huge hump, also largely due to interchannel interactions with the $5d$ channels. At higher energies, a second induced minimum appears (seen clearly in the inset in Fig. 5) owing to interchannel coupling with $5p$; the $5p$ channels are just opening in the vicinity of the minimum. Thus, as was the case for Ra $7s$, the $6s$ cross sections in Ra and Rn are dominated by interchannel coupling.

This interchannel coupling also dominates the energy dependence of the β parameter, as seen in Fig. 6. Recalling that, for a closed-shell atom, $\beta=2$ for s subshells independent of energy in the absence of relativistic effects, it is clear from Fig. 6 that relativistic effects are extremely important in these cases. For reasons discussed in connection with Ra $7s$, β should approach -1 in the vicinity of minima. This is indeed what is seen near threshold and in the 7–8 a.u. range for Ra and Rn $6s$, confirming that the interpretation of the cross sections in terms of induced minima was indeed correct. Away from these minima, β tends toward 2, as expected.

D. 5d subshells

The $5d$ subshell cross sections for Ra and Rn are shown in Fig. 7. Note that the cross sections are not shown down to threshold because the computer codes showed some instabilities in this region. Nevertheless, it is clear that the $5d$ cross sections are large near threshold, over 30 Mb, and seem to drop off in a monotonic fashion. This is not really true, as the inset in Fig. 7 shows; a minimum clearly exists around 10 a.u. Similar

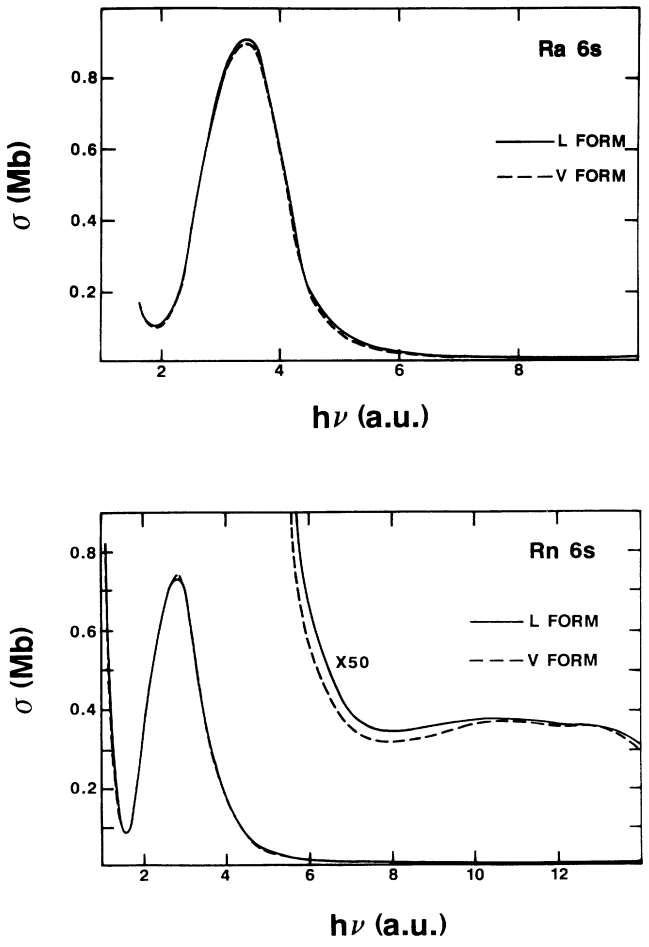

FIG. 5. Photoionization cross section for Ra $6s$ calculated in a 20-channel RRPA and Rn $6s$ calculated in an 18-channel RRPA in dipole-length (L) and dipole-velocity (V) formulations.

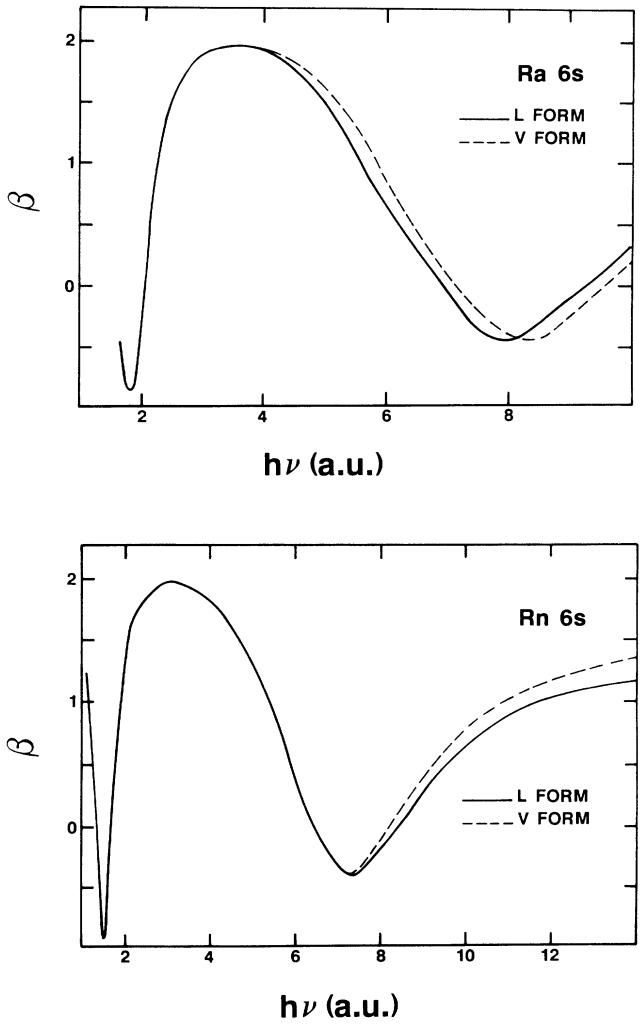

FIG. 6. Photoelectron angular-distribution asymmetry parameter β for Ra $6s$ calculated in a 20-channel RRPA and Rn $6s$ calculated in a 18-channel RRPA in dipole-length (L) and dipole-velocity (V) formulations.

scrutiny (not shown) reveals the same sort of effect for Ra $5d$, but at somewhat higher energy.

These minima are intrinsic as they appear in the DS calculation [4]. But the $5d$ cross sections show no induced minima in the energy range we have studied, in contrast to all of the subshells previously discussed. This is because interchannel coupling effects are strong on a weak channel when it is degenerate with a strong one, i.e., when a channel has a small cross section, mixing in a small fraction of a channel with a much larger cross section can change the small cross section considerably. But, if a channel is strong, mixing in smaller channels will have no appreciable effect. For example, the Ra $7s$ cross section is a few tenths of a megabarn when the $6p$ channels open with threshold cross section more than 10 Mb; similarly, when the $5d$ channels open at $\sim$30 Mb near threshold. Thus, the Ra $7s$ cross section is strongly affected by $6p$ and $5d$, but not by $6s$ which was seen to be similarly small. On the other hand, the $5d$ cross section is much larger than the cross sections of the higher subshells for both Ra and Rn, and even when the $5p$ channels open, it will be seen in the next subsection that the $5p$ cross sections are not large compared to $5d$ at those energies. Thus, no appreciable interchannel effects on the $5d$ cross sections are shown in Fig. 7.

The relativistic splitting of the $5d \rightarrow \epsilon f$ Cooper minima for Rn is found to be about 1.5 a.u., which is about a factor of 10 larger than the Rn $5d$ spin-orbit splitting of 0.17 a.u. from Table I, and we find a similar result for Ra. Contrast this factor of 10 with the factor of 30 found in the $6p$ case, discussed in Sec. II B. This is a consequence of the relative strengths of the centrifugal barrier in initial and final states of the photoionizing transition. Since the magnification of the splitting occurs because the centrifugal barrier is stronger in the final continuum state than the initial discrete state, the ratio of final-state to initial-state barrier strengths, $l(l+1)$ is of importance. For $p \rightarrow d$ transitions this ratio is 3, while for $d \rightarrow f$ it is 2. Thus, we expect the magnification effect to be smaller for $d \rightarrow f$ transitions than for $p \rightarrow d$, just as the calculations show.

The $5d$ β parameters are shown in Fig. 8 for Ra and Rn respectively. These β's behave quite smoothly compared to the $7s$, $6p$, and $6s$ β's discussed above. This, of

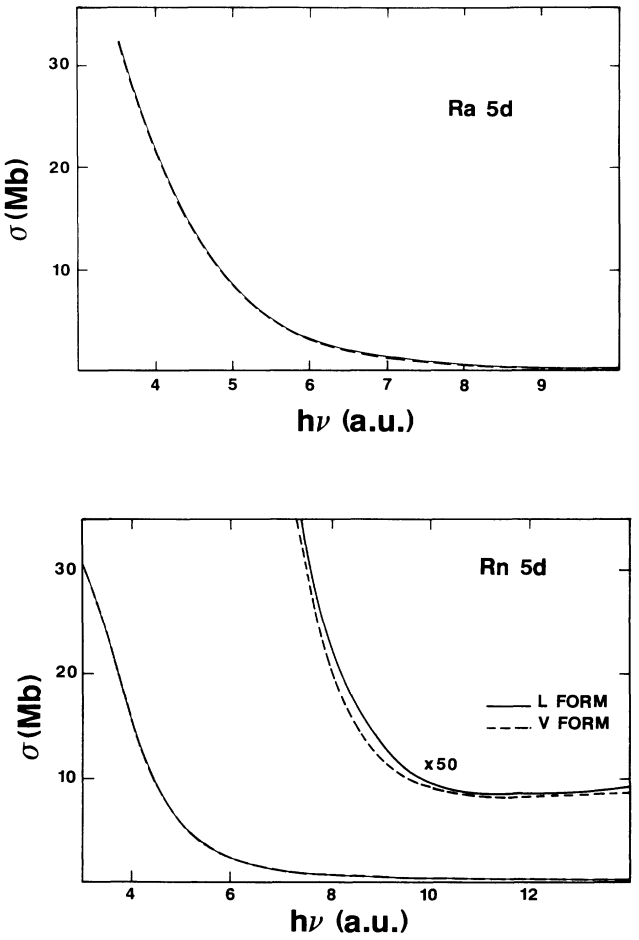

FIG. 7. Photoionization cross section for Ra $5d$ calculated in an 18-channel RRPA and Rn $5d$ calculated in an 18-channel RRPA in dipole-length (L) and dipole-velocity (V) formulations.

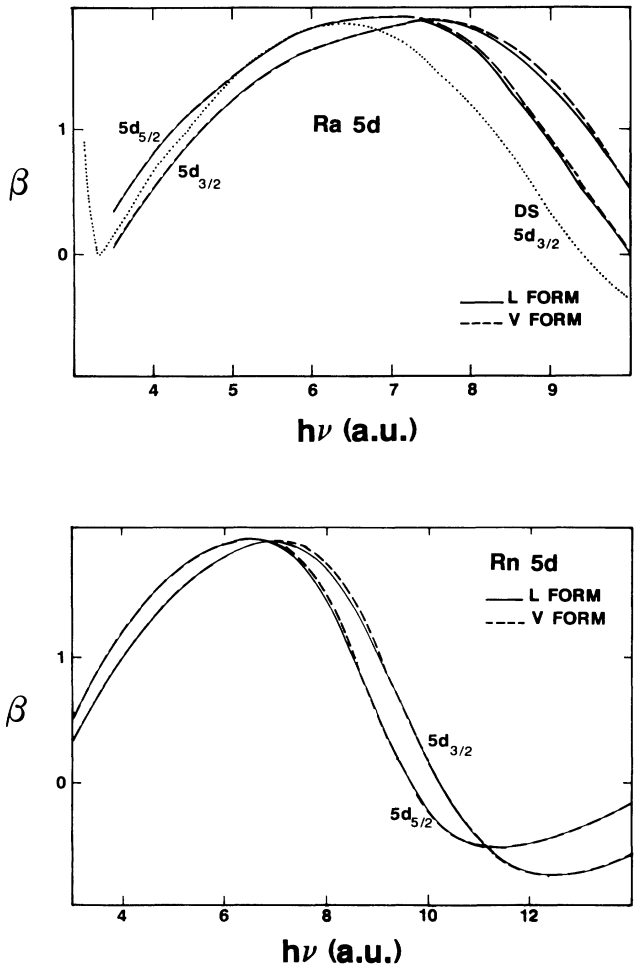

FIG. 8. Photoelectron angular-distribution asymmetry parameter β for Ra $5d_{5/2}$ and $5d_{3/2}$ calculated in a 20-channel RRPA and Rn $5d_{5/2}$ and $5d_{3/2}$ calculated in an 18-channel RRPA in dipole-length (L) and dipole-velocity (V) formulations. The dotted curve is the DS $5d_{3/2}$ result of Ref. [4].

course, is because there are no induced minima in the lower-energy region as there are in other cases. Rapid variation is seen to occur, however, at the higher energies in the vicinity of the Cooper minima. At the point where the $d \rightarrow f$ contribution goes to zero (which never quite happens for $d_{5/2}$ since $d_{5/2} \rightarrow f_{7/2}$ and $d_{5/2} \rightarrow f_{5/2}$ vanish at different energies) $\beta = 1/5$. From Fig. 8 it is seen that the β's do approach $\frac{1}{5}$ in the neighborhood of the Cooper minima. The splitting between the β's for $5d_{5/2}$ and $5d_{3/2}$, in the region of the minima, is a direct result of the splitting of the minima; this splitting increases with Z as the DS model predicted [4].

Also shown in Fig. 8 is the DS result for the $5d_{3/2}\beta$. While we cannot compare just at threshold, agreement with the RRPA result is quite good in the 3–6 a.u. region. At higher energies, the DS β drops too rapidly, indicating that the DS calculation predicts a Cooper minimum in the $5d_{3/2} \rightarrow \epsilon f_{5/2}$ channel which is too low in energy. We expect, however, that well above the Cooper minima, agreement will again be good.

The $5d$ branching ratios γ are shown in Fig. 9 for Ra and Rn. At low energies, the fact that the cross section is decreasing, along with the fact that the $5d_{5/2}$ minima occur at a lower energy than the $5d_{3/2}$, combine to insure that γ, in both cases, lies below the statistical value of 1.5. With increasing energy, the γ's drop further as we go through the $5d_{5/2}$ minima, making the $5d_{5/2}$ cross section anomalously small compared to the $5d_{3/2}$. At still higher energies, the γ's start to rise, as the $5d_{5/2}$ cross section is recovering from its minima, while the $5d_{3/2}$ is still dropping toward its minima. This is as high in energy as we have calculated for Ra $5d$, but for Rn, above the $5d_{3/2} \rightarrow \epsilon f_{5/2}$ minimum, which occurs at about 10.5 a.u., the $5d_{3/2}$ cross section starts to recover and γ, while going above statistical since the $5d_{3/2}$ cross section remains anomalously small, is seen to begin to level off. It is interesting to note that these results are quite similar to the DS results [4] on a qualitative level; however, the fact that the DS minima are off means that the DS γ's are correspondingly inaccurate.

E. 5p subshells

The omission of the region between threshold of the spin-orbit doublets was seen to be of not much conse-

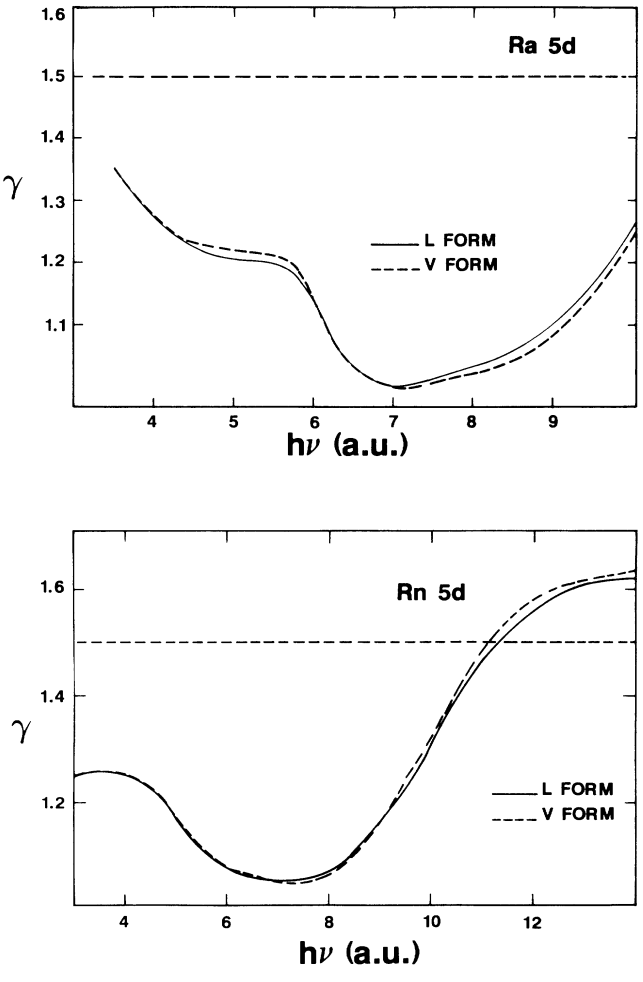

FIG. 9. $5d_{5/2}$:$5d_{3/2}$ branching ratio γ for Ra $5d$ calculated in a 20-channel RRPA and Rn $5d$ calculated in an 18-channel RRPA in dipole-length (L) and dipole-velocity (V) formulations. The dashed line is the statistical ratio of 1.5.

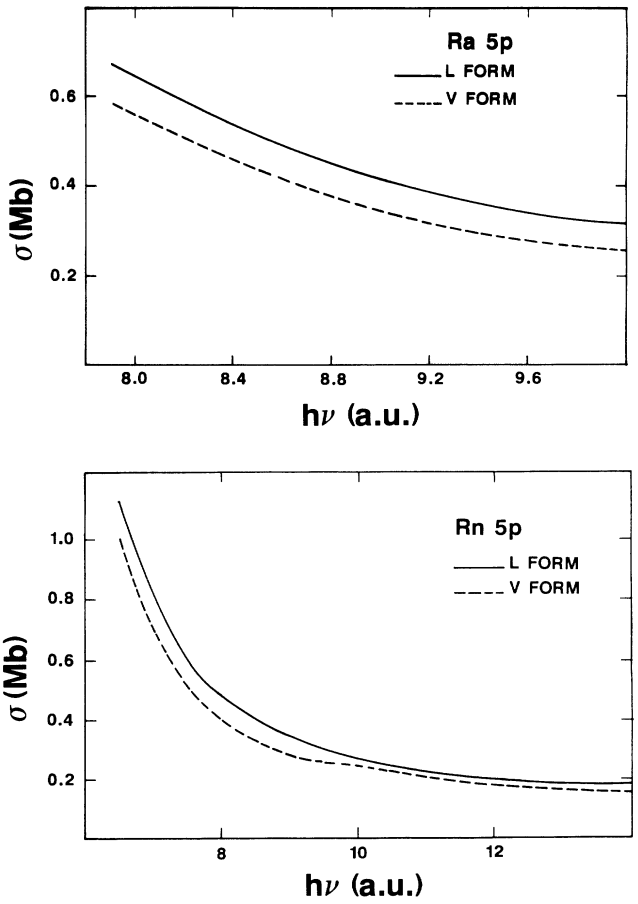

FIG. 10. Photoionization cross section for Ra $5p$ calculated in a 20-channel RRPA and Rn $5p$ calculated in an 18-channel RRPA in dipole-length (L) and dipole-velocity (V) formulations.

quence for the $6p$ subshells, and only slightly more for $5d$; for $5p$ this omission is of major importance since the thresholds are so widely separated, 1.23 a.u. for Rn and 1.47 a.u. for Ra as seen from Table I. This, combined with a cutoff of the calculations in the neighborhood of the next inner threshold means that only a small portion of the $5p$ cross sections have been calculated, i.e., in contrast to the other subshells studied, only a small fraction of the $5p$ oscillator strength is represented in each case, although somewhat more for Rn.

The cross sections obtained for $5p$ photoionization are shown in Fig. 10 where it is seen that length and velocity show notable differences even at the lowest energies considered in each case. Clearly this is due to the truncation of the RRPA calculation—the omission of channels arising from $5s$, $4f$, $4d$, etc. Cooper minima appear in the calculations, even in the restricted energy region considered; although they do not show up as minima in the total subshell cross section, these minima affect the β's and γ's strongly. The $5p_{3/2} \rightarrow \epsilon d$ minima in Ra and Rn are in the 8–9 a.u. range, while the $5p_{1/2} \rightarrow \epsilon d_{3/2}$ channels show indications of a minima at *much* higher energy. The locations of the $5p$ minima must be considered tentative, however, since the interchannel interactions omitted could alter the situation markedly.

The β's obtained are given in Fig. 11. In each case, $5p_{3/2}$ goes through zero, indicating the presence of Cooper minima; the exact location of the zeros show that the Cooper minima are moving to larger $h\nu$, with increasing Z, just like the higher subshells and the DS prediction [14]. The $5p_{1/2}$ β's, on the other hand, do not pass through zero over the energy considered confirming that there is no $5p_{1/2} \rightarrow \epsilon d_{3/2}$ minimum in this range, although it seems close in Rn. It is clear from Fig. 11, however, that there is a huge splitting of the β's for both Ra and Rn. It is also interesting to note that the length and velocity results are much closer together for the β's than for the γ's; the ratios involved in the calculation of β apparently tend to cancel the differences out.

The $5p$ branching ratios are shown in Fig. 12 where a monotonically increasing γ is seen, in each case, starting from well below the statistical ratio of 2. The low γ for the lowest energies is the result of the $5p_{3/2}$ Cooper minima; the subsequent rise is a consequence of the $5p_{1/2}$ cross section dropping toward its minimum while the $5p_{3/2}$ is recovering. Differences between length and ve-

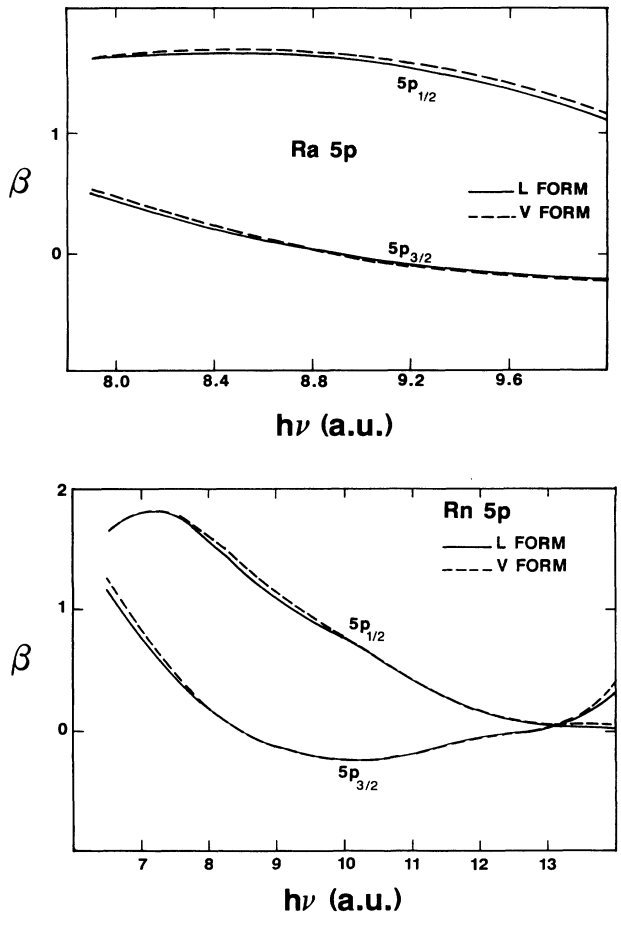

FIG. 11. Photoelectron angular-distribution asymmetry parameter β for $5p_{3/2}$ and $5p_{1/2}$ of Ra calculated in a 20-channel RRPA and Rn calculated in an 18-channel RRPA in dipole-length (L) and dipole-velocity (V) formulations. The dotted curve is the DS $5d_{3/2}$ result of Ref. [4].

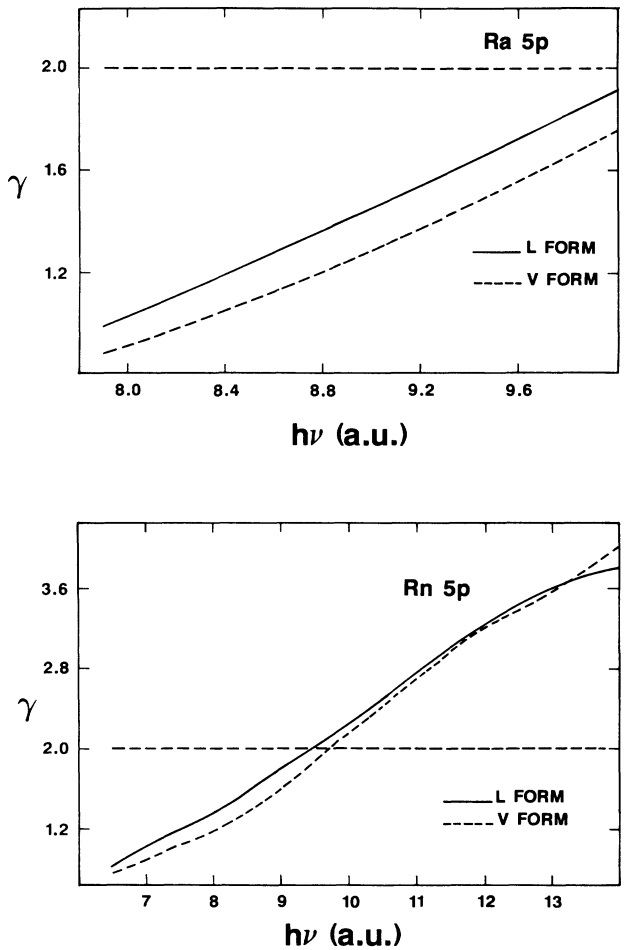

FIG. 12. $5p_{3/2}$:$5p_{1/2}$ branching ratio γ for Ra $5p$ calculated in a 20-channel RRPA and Rn calculated in an 18-channel RRPA in dipole-length (L) and dipole-velocity (V) formulations. The dashed line is the statistical ratio of 2.0.

locity are substantially as large as were seen for the $5p$ cross sections. Clearly the canceling out that occurred for β within the $5p_{1/2}$ and $5p_{3/2}$ channels does not occur for γ which is a ratio between the $5p_{3/2}$ and $5p_{1/2}$ channels.

III. CONCLUDING REMARKS

The cross sections, photoelectron angular-distribution asymmetry parameters, and branching ratios have been calculated for the outer subshells of the high-Z elements Ra and Rn within the framework of RRPA. The results confirm qualitatively previous work based on the central-field DS approximation [3,4], which predicted huge splittings in the positions of Cooper minima in the dipole matrix elements under the action of relativistic (notably spin-orbit) effects. Quantitatively, the details of the DS predictions are altered significantly by RRPA. In addition, a number of minima in dipole matrix elements induced by interchannel coupling were found. These induced minima are physically no different from intrinsic Cooper minima; they simply do not appear in ordinary single-particle calculations. Note that the relativistic interactions are not required to induce minima [20]; they only increase the number via spin-orbit splittings. The existence and location of these various minima are found to be the principle determinants of the spectral distribution of oscillator strength in the photoionization cross sections, and even more so for the β's and γ's. Dramatic differences of the β's of the spin-orbit doublets and deviation of the γ's from statistical ratios are seen to result from these minima.

As mentioned, interchannel interactions are responsible for induced minima in dipole matrix elements, but interchannel interactions produce other structures and generally modify the spectral distribution of oscillator strength as well. From the experience with Ra and Rn, it is found that the cross section for a particular channel at a given energy is modified significantly by interchannel coupling with channels with much larger cross sections at that same energy. This rule, which follows the intuition, should be true generally.

And where do we go from here? From the theory side, looking at the resonance regions and at higher energies (at least to complete the study of $5p$) seems to be necessary. In addition, it would be extremely useful to look at some of these cross sections with another sophisticated calculation to get some idea as to how the results would be modified by non-RPA correlations. On the experimental side, it would be extremely useful to have some experimental data on photoionization at such high Z; at present none has been reported.

ACKNOWLEDGMENTS

We are very grateful to Professor Walter R. Johnson, University of Notre Dame, for giving us his computer codes for these studies. This work was supported in part by the National Science Foundation and in part by the United States Army Research Office.

[1] C. E. Theodosiou, A. F. Starace, B. R. Tambe, and S. T. Manson, Phys. Rev. A **24**, 301 (1981); B. R. Tambe, W. Ong, and S. T. Manson, *ibid.* **23**, 799 (1981).

[2] W. R. Johnson, V. Radojević, P. Deshmukh, and K. T. Cheng, Phys. Rev. A **25**, 337 (1982); W. R. Johnson and V. Radojević, Phys. Lett. **92A**, 75 (1982); V. Radojević and W. R. Johnson, *ibid.* **97A**, 335 (1983).

[3] Y. S. Kim, A. Ron, R. H. Pratt, B. R. Tambe, and S. T. Manson, Phys. Rev. Lett. **46**, 1326 (1981); S. T. Manson, C. J. Lee, R. H. Pratt, I. B. Goldberg, B. R. Tambe, and A. Ron, Phys. Rev. A **28**, 2885 (1983).

[4] B. R. Tambe and S. T. Manson, Phys. Rev. A **30**, 256 (1984).

[5] P. C. Deshmukh, V. Radojević, and S. T. Manson, Phys. Lett. **117**, 293 (1986).

[6] P. C. Deshmukh, V. Radojević, and S. T. Manson, Phys. Rev. A **34**, 5162 (1986).

[7] W. R. Johnson, C. D. Lin, Phys. Rev. A **20**, 964 (1979).

[8] W. R. Johnson, C. D. Lin, K. T. Cheng, and C. M. Lee, Phys. Scr. **21**, 409 (1980).

[9] W. R. Johnson and K. T. Cheng, Phys. Rev. A **20**, 978 (1979).

[10] P. C. Deshmukh and W. R. Johnson, Phys. Rev. A **27**, 326 (1983).

[11] J. W. Cooper, Phys. Rev. **128**, 681 (1962).

[12] S. T. Manson, and J. W. Cooper, Phys. Rev. **165**, 126 (1968).

[13] S. T. Manson, Phys. Rev. A **31**, 3698 (1985).

[14] R. Y. Yin and R. H. Pratt, Phys. Rev. A **35**, 1149 (1987).

[15] C. M. Lee and W. R. Johnson, Phys. Rev. A **22**, 979 (1980).

[16] P. C. Deshmukh, V. Radojević, and S. T. Manson, Phys. Lett. A **117**, 293 (1986).

[17] S. T. Manson and A. F. Starace, Rev. Mod. Phys. **54**, 389 (1982).

[18] Y. S. Kim, R. H. Pratt, A. Ron, and H. K. Tseng, Phys. Rev. A **22**, 567 (1980).

[19] T. E. H. Walker and J. T. Waber, J. Phys. B **6**, 1165 (1973).

[20] M. Ya Amusia and N. A. Cherepkov, Case Stud. At. Phys. **5**, 47 (1975), and references therein.